Progress In Electromagnetics Research M, Vol. 35, 77–86, 2014

Study of Whistler Mode Wave by Injection of Relativistic Hot Electrons Beam in the Magnetosphere of Uranus

Rama S. Pandey and Rajbir Kaur*

Abstract—In present paper, the effect of relativistic hot electron beam for field aligned Whistler mode waves has been studied theoretically in the presence of AC electric field perpendicular to magnetic field. Studies have been performed using perturbative approach along with the method of characteristic solutions and are valid for comparatively small ambient magnetic field of Uranus, of the order of nano Tesla, as observed by Voyager 2. The detailed derivation and calculations has been done for dispersion relation and growth rate for magnetosphere of Uranus. Analyses are done by changing various plasma parameters which are explained in result and discussions section of this paper. Extensive study of wave-particle interactions and numerical calculations concludes that in case of injection of a distribution of particles having a positive slope in $v_\perp$, temperature anisotropy remains the main source of free energy. It is seen that other effective parameters for the growth of whistler mode waves are AC frequency and higher number density of hot electrons. We also learn that even the minimal presence of such energetic particles having a positive slope of distribution function and increasing power of perpendicular thermal velocity can increase the growth rate significantly in the magnetosphere of Uranus. The present work is basically based upon the theoretical investigation and mathematical analysis of the magnetosphere of Uranus, supported by satellite data.

1. INTRODUCTION

Extensive theoretical analyses and laboratory studies show that waves play dominant roles in all non-equilibrium plasma systems [1, 2]. Especially when plasma is dilute and cool, regular Coulombic collisions become less important, and wave-particle interactions provide the scattering and accelerating mechanisms that govern the dynamics. Wave investigations in magnetized planet's orbit have demonstrated that two general classes of wave-particle interactions control important aspects of plasma dynamics in magnetospheres. Electromagnetic and electrostatic plasma instabilities give rise to narrow banded spontaneous emissions. Such emissions, e.g., ELF hiss, chorus, three-halves noise, ion cyclotron and ion-plasma-frequency turbulence, scatter trapped particles into the loss cone, leading to modified pitch-angle distributions, stable trapping limits, diffuse aurora etc.. The current-driven plasma instabilities generate intense impulsive ion acoustic mode turbulence that provides very effective energy transfer at the bow shock and in regions where strong field-aligned currents are observed [3].

Studies of wave-particle interaction phenomena in the outer magnetospheres are of great importance. These outer regions are dominated by high β plasma spun out by centrifugal forces and here wave-particle interactions provide local acceleration. These affect particle diffusion and can lead to field-line merging [3]. Other relevant wave-particle interactions involve whistlers generated by atmospheric lightening and electron plasma oscillations associated with suprathermal particles in the upstream solar wind. Such whistler mode waves have been observed in the magnetosphere of Jupiter and Uranus [4–8] and in the solar wind upstream of Mercury, Venus, Earth and Saturn [9].

Received 2 January 2014, Accepted 11 February 2014, Scheduled 3 March 2014

* Corresponding author: Rajbir Kaur (rkaur2@amity.edu).
The authors are with the Department of Applied Physics, Amity Institute of Applied Sciences, Amity University, Sector-125, Noida, UP, India.

Voyager 2 encounter of Uranus on 24 January 1986 revealed a strong planetary magnetic field, an associated magnetosphere and fully bipolar magnetic tail of Uranus. The results from Voyager 2 plasma wave instrument (PWS) show radio emissions from Uranus about 5 days before the closest approach at frequencies 31.1 and 56.2 kilohertz and then about 10 hours before closest approach the bow shock was identified [10]. A maximum magnetic field of 413 nanotesla was observed at 4.19 R_U, just before the closest approach [11]. The instrument also detected that inner magnetosphere is characterized by both the types of strong whistler mode emissions, chorus and hiss. Chorus and hiss are produced by cyclotron resonance interaction with energetic electrons. These waves were identified as whistler-mode on the basis of the frequency range, which is always below electron cyclotron frequency ($f_c = 28B$ Hz, where B is magnetic field intensity in units of nanotesla). Hudson et al. [12] and Clark et al. [13] investigated the process of generation of electric field in the magnetosphere of Uranus and reported its magnitude as used by Pandey et al. [14] in their theoretical magnetospheric studies. In magnetosphere and in shock regions, AC electric field observations have been reported perpendicular and along the magnetic field [15].

In last few decades, many research rockets and space vehicles have injected electron beams into the ionosphere and magnetosphere. Particle beams provide a unique way to study numerous problems in basic space plasma physics. Electron beams act as tracers in the large-scale magnetosphere and also generate waves, plasma heating and current systems [16]. Examples from Echo program are used to illustrate electron beams as 'magnetospheric probes'. Several types of experiments search for beam echoes from field-aligned potential differences thought to cause auroras. The injection of such beams creates rich sources of plasma and electromagnetic waves. The frequency range includes lower hybrid, whistler mode, upper hybrid, electron cyclotron harmonics and plasma frequency emissions [17]. Winglee and Kellogg [18] explained the spectra generated from the Echo 7 experiment. The results showed that characteristics of emissions can change substantially with altitude. Relativistic electromagnetic particle simulations were used to investigate the changes in plasma conditions. It was shown that many variations could be accounted for by assuming that the ratio of the electron plasma frequency to cyclotron frequency is less than unity at the lower altitudes of about 200 km and near or above unity at apogee of about 300 km. It was concluded that in the lower altitude case, whistlers with a cutoff at ωpe, lower hybrid and plasma waves are driven by the parallel beam energy while electromagnetic fundamental z mode and second harmonic x mode and electrostatic upper hybrid waves are driven by the perpendicular beam energy through the maser instability at higher altitudes.

Inspired from above literature, whistler mode waves have been studied theoretically in this paper. As Pandey et al. [19] studied the effect of cold plasma injection on whistler mode instability triggered by perpendicular AC electric field at Uranus, we will investigate whistler mode waves by injection of hot electron beam in the magnetosphere of Uranus. In this paper, the beam particles considered hot due to thermal anisotropy and relativistic effect. Also the relativistic effect of beam, affecting the velocity of beam particles, will also be studied while considering the presence of perpendicular AC electric field to magnetic field and by using the method of characteristic solutions and kinetic approach, the detailed derivation and calculations has been done for dispersion relation and growth rate for magnetosphere of Uranus. Parametric analysis has been done by changing various plasma parameters: temperature anisotropy, AC frequency, ratio of n_c/n_w and relativistic factor to study their effects in the magnetosphere of Uranus.

2. DISPERSION RELATION AND GROWTH RATE

A homogeneous anisotropic collisionless plasma in the presence of an external magnetic field $B_0 = (B_0 e_z)$ and an electric field $E_{ox} = E_o \sin vt e_x$ is assumed. In interaction zone inhomogeneity is assumed to be small. In order to obtain the particle trajectories, perturbed distribution function and dispersion relation, the linearised Vlasov-Maxwell equations are used. Separating the equilibrium and non equilibrium parts, neglecting the higher order terms and following the techniques of Pandey et al. [19] the linearized Vlasov equations are given as:

$$\mathrm{v} \cdot \left(\frac{\delta f_0}{\delta r}\right) + \left(\frac{e_s}{m_e}\right)\left[E_0 \sin vt + \frac{(\mathrm{v} \times B_0)}{c}\right] \cdot \left(\frac{\delta f_0}{\delta v}\right) = 0 \tag{1}$$

$$\left(\frac{\delta f_1}{\delta t}\right) + v \cdot \left(\frac{\delta f_1}{\delta r}\right) + \left(\frac{F}{M_e}\right) \cdot \left(\frac{\delta f_1}{\delta v}\right) = S\left(r, \mathrm{v}, t\right) \tag{2}$$

where the force

$$F = e\left[E_0 \sin \upsilon t + \frac{(\mathrm{v} \times B_0)}{c}\right] = m\frac{d\mathrm{v}}{dt} \tag{3}$$

where υ is AC frequency and the dispersion relation is defined as

$$S(r, \mathrm{v}, t) = -\left(\frac{e_s}{m_e}\right)\left[E_1 + \frac{(\mathrm{v} \times B_0)}{c}\right] \cdot \left(\frac{\delta f_0}{\delta v}\right) \tag{4}$$

where s denotes the type of electrons. Subscript '0' denotes the equilibrium values. The perturbed distribution function f_1 is determined by using the method of characteristic, which is

$$f_1(r, \mathrm{v}, t) = \int_0^\infty S\left\{r_0\left(r, \mathrm{v}, t\right), v_0\left(r, \mathrm{v}, t\right), t - t'\right\} dt$$

we have transformed the phase space coordinate system for $(r,\ v,\ t)$ to $(r_0,\ v_0,\ t - t')$. The relativistic particle trajectories that have been obtained by solving Equation (3) for given external field configuration are

$$\begin{aligned}
X_0 &= X + \left(\frac{P_\perp \sin\theta}{\omega_c m_c}\right) - \left[P_\perp \sin\left\{\frac{\theta + \left(\dfrac{\omega_c t}{\beta}\right)}{\omega_c m_c}\right\}\right] + \left[\frac{\Gamma_x \sin \upsilon t}{\beta\left\{\left(\dfrac{\omega_c}{\beta}\right)^2 - \upsilon^2\right\}}\right] - \left[\frac{\upsilon\Gamma_x \sin\left(\dfrac{\omega_c t}{\beta}\right)}{\omega_c\left\{\left(\dfrac{\omega_c t}{\beta}\right) - \upsilon^2\right\}}\right] \\
Y_0 &= Y - \left(\frac{P_\perp \cos\theta}{\omega_c m_c}\right) - \left[P_\perp \cos\left\{\frac{\theta + \left(\dfrac{\omega_c t}{\beta}\right)}{\omega_c m_c}\right\}\right] + \left(\frac{\Gamma_x}{\upsilon\omega_c}\right) - \frac{\left\{1 + \upsilon^2\beta^2 \cos\left(\dfrac{\omega_c t}{\beta}\right) - \omega_c^2 \cos \upsilon t\right\}}{\beta^2\left\{\left(\dfrac{\omega_c}{\beta}\right)^2 - \upsilon^2\right\}} \\
z_0 &= z - \frac{P_z}{\beta m_e}
\end{aligned} \tag{5}$$

and the velocities are

$$\begin{aligned}
\mathrm{v}_{xo} &= P_\perp \cos\left\{\theta + \frac{\left(\dfrac{\omega_c t}{\beta}\right)}{\beta m_e}\right\} + \left[\frac{\upsilon\Gamma_x}{p\left\{\left(\dfrac{\omega_c}{\beta}\right)^2 - \upsilon^2\right\}}\right]\left\{\cos \upsilon t - \cos\left(\frac{\omega_c t}{\beta}\right)\right\} \\
\mathrm{v}_{yo} &= P_\perp \sin\left\{\theta + \frac{\left(\dfrac{\omega_c t}{\beta}\right)}{\beta m_e}\right\} + \left[\frac{\Gamma_x}{\beta\left\{\left(\dfrac{\omega_c}{\beta}\right)^2 - \upsilon^2\right\}}\right]\left\{\left(\frac{\omega_c}{\beta}\right)\sin \upsilon t - \upsilon \sin\left(\frac{\omega_c t}{\beta}\right)\right\} \\
\mathrm{v}_{zo} &= \frac{P_z}{\beta m_e} \\
\mathrm{v}_x &= \frac{P_\perp \cos\theta}{\beta m_e}, \quad \mathrm{v}_y = \frac{P_\perp \sin\theta}{\beta m_e}, \quad \mathrm{v}_z = \frac{P_z}{\beta m_e} \\
\Gamma_x &= \frac{eE_o}{m_e}, \quad m_e = \frac{m_s}{\beta}, \quad \beta = \sqrt{1 - \frac{v^2}{c^2}}, \quad \omega_c = \frac{eB_0}{m_e}
\end{aligned} \tag{6}$$

$P_\perp$ and P_z denote momenta perpendicular and parallel to the magnetic field. Using Equations (6), (7) and the Bessel identity and performing the time integration, following the technique and method of Misra and Pandey [20], the perturbed distribution function is found after some lengthy algebraic simplifications as:

$$f_1 = -\left(\frac{ie_s}{me\beta\omega}\right)\sum J_s\left(\lambda_3\right)\exp i(m-n)\theta\left[\frac{J_mJ_nJ_pU^*E_{1x} - iJ_mV^*E_1 + J_mJ_nJ_pW^*}{\omega - \left(\frac{k_{||}P_z}{\beta m_e} + p\upsilon - \frac{(n+g)\,\omega_c}{\beta}\right)}\right] \tag{7}$$

Due to the phase factor the solution is possible when $m = n$. Here,

$$\begin{aligned}
U^* &= \left(\frac{c_1P_\perp n}{\beta\lambda_1 m_e}\right) - \left(\frac{n\upsilon c_1 D}{\lambda_1}\right) + \left(\frac{p\upsilon c_1 D}{\lambda_2}\right)\\
V^* &= \left(\frac{c_1P_\perp J_nJ_p}{\beta\lambda_1 m_e}\right) + c_1DJ_pJ_n\omega_c\\
W^* &= \left(\frac{n\omega_cFm_e}{k_\perp P_\perp}\right) + \left(\frac{\beta m_eP_\perp\omega\partial f_0}{\partial P_z}\right) + G\left\{\left(\frac{p}{\lambda_2}\right) - \left(\frac{n}{\lambda_1}\right)\right\}\\
C_1 &= \left\{\frac{(\beta m_e)}{P_\perp}\right\}\left(\frac{\partial f_0}{\partial P_\perp}\right)\left(\omega - \frac{k_{||}P_z}{\beta m_e}\right) + k_{||}\beta m_e\left(\frac{\partial f_0}{\partial P_\perp}\right)\\
D &= \left[\frac{\Gamma_x}{\beta\left\{\left(\frac{\omega_c}{\beta}\right)^2 - \upsilon^2\right\}}\right], \quad F = \frac{Hk_\perp P_\perp}{\beta m_e}\\
H &= \left\{\frac{(\beta m_e)^2}{P_\perp}\right\}\left(\frac{\partial f_0}{\partial P_\perp}\right)\left(\frac{P_z}{\beta m_e}\right) + \beta m_e\left(\frac{\partial f_0}{\partial P_z}\right), \quad G = \frac{Hk_\perp\upsilon\Gamma_x}{\beta\left\{\left(\frac{\omega_c}{\beta}\right)^2 - \upsilon^2\right\}}
\end{aligned} \tag{8}$$

$$J_n'(\lambda_1) = \frac{dJ_n(\lambda_1)}{d\lambda_1} \quad \text{and} \quad J_p'(\lambda_2) = \frac{dJ_p(\lambda_2)}{d\lambda_2}$$

The Bessel function arguments are defined as

$$\lambda_1 = \frac{k_\perp P_\perp}{\omega_c m_e}\frac{k_\perp\Gamma_x}{\beta\left\{\left(\frac{\omega_c}{\beta}\right)^2 - \upsilon^2\right\}} \quad \text{and} \quad \lambda_3 = \frac{k_\perp\upsilon\Gamma_x}{\beta\left\{\left(\frac{\omega_c}{\beta}\right)^2 - \upsilon^2\right\}}$$

The conductivity tensor $||\sigma||$ is found to be

$$\|\sigma\| = \frac{-i\sum\left(e^2/\beta m_e\right)^2\omega\int d^3P J_g\left(\lambda_3\right)||s||}{\left[\omega - \left(\frac{k_{||}P_z}{\beta m_e}\right) - \left((n+g)\,\frac{\omega_c}{\beta}\right) + p\upsilon\right]}$$

where

$$||S|| = \begin{vmatrix} P_\perp J_n^2J_p\left(\frac{n}{\lambda_1}\right)U^* & iP_\perp J_nV^* & P_\perp J_n^2J_p\left(\frac{n}{\lambda_1}\right)W^*\\ P_\perp J_n'J_nJ_p\left(\frac{n}{\lambda_1}\right)U^* & iP_\perp J_n'V^* & P_\perp J_n'J_p\left(\frac{n}{\lambda_1}\right)W^*\\ P_zJ_n^2J_p\left(\frac{n}{\lambda_1}\right)U^* & iP_zJ_nV^* & P_zJ_n^2J_p\left(\frac{n}{\lambda_1}\right)W^* \end{vmatrix}$$

By using these in the Maxwell's equations we get the dielectric tensor,

$$\varepsilon_{ij} = 1 + \sum \left\{ \frac{4\pi e_s^2}{(\beta m_e)^2 \omega} \right\} \int \frac{d^3 P J_g(\lambda_3) ||S||}{\left(\omega - \frac{k_{||} P_z}{\beta m_e}\right) - \left\{ \frac{(n+g)\omega_c}{\beta} \right\} + pv}$$

For parallel propagating whistler mode instability, the general dispersion relation reduces to $\varepsilon_{11} \pm \varepsilon_{12} = N^2$ where $N^2 = \frac{k^2 c^2}{\omega^2}$.

The dispersion relation for relativistic case with perpendicular AC electric field for $g = 0$, $p = 1$, $n = 1$ is written as:

$$\begin{aligned} \frac{k^2 c^2}{\omega^2} &= 1 + \frac{4\pi e_s^2}{(\beta m_e)^2 \omega^2} \int \frac{d^3 P}{\beta} \left[\frac{P_\perp}{2} - \frac{\upsilon \Gamma_x m_e}{2\left(\frac{\omega_c^2}{\beta^2} - \upsilon^2\right)} \right] \\ &\quad \left[\left(\beta\omega - \frac{k_{||} P_{||}}{m_e}\right)^2 \frac{\partial f_0}{\partial P_\perp} + \frac{P_\perp k_{||}}{m_e} \frac{\partial f_0}{\partial P_\perp} \right] \frac{1}{\beta\omega - \frac{k_{||} P_{||}}{m_e} - \omega_c + \beta\upsilon} \end{aligned} \tag{9}$$

The generalization distribution function [21] is given as

$$f_0 = \left\{ n_o P_\perp^{2j} / \pi^{3/2} P_{o\perp}^{2(j+1)} P_{o\perp} j! \right\} \exp\left[(-P_\perp / P_{o\perp})^2 - \left(P_{||} / P_{o||}\right)^2 \right] \tag{10}$$

where $P_{o\perp}$ and $P_{o||}$ are perpendicular and parallel momenta for a temperature T. Substituting $4\pi e_s^2 n_o / m_e = \omega_p^2$ and integrating Equation (9) by parts, the dispersion relation is found as

$$\frac{k^2 c^2}{\omega^2} = 1 - \frac{\omega_p^2}{\omega^2} \int \frac{d^3 P}{\beta} \left[1 - \frac{\upsilon \Gamma_x m_e}{P_\perp \left(\frac{\omega_c^2}{\beta^2} - \upsilon^2\right)} \right] \left[\frac{\left(\beta\omega - \frac{k_{||} P_{||}}{m_e}\right)}{\left(\beta\omega - \frac{k_{||} P_{||}}{m_e} - \omega_c + \beta\upsilon\right)} - \frac{P_\perp^2}{2 m_e^2 c^2} \frac{\left(\omega^2 - k_{||}^2 c^2\right)}{\left(\beta\omega - \frac{k_{||} P_{||}}{m_e} - \omega c + \beta\upsilon\right)^2} \right] f_o \tag{11}$$

When we remove AC field and set $j = 0$ for bi-Maxwellian only, the relation becomes similar to [22]

$$\frac{k^2 c^2}{\omega^2} = 1 - \frac{\omega_p^2}{\omega^2} \int \frac{d^3 P}{\beta} \left[\frac{\left(\beta\omega - \frac{k_{||} P_{||}}{m_e}\right)}{\left(\beta\omega - \frac{k_{||} P_{||}}{m_e} - \omega_c\right)} - \frac{P_\perp^2}{2 m_e^2 c^2} \frac{\left(\omega^2 - k_{||}^2 c^2\right)}{\left(\beta\omega - \frac{k_{||} P_{||}}{m_e} - \omega_c\right)^2} \right] f_o \tag{12}$$

Using Equations (10) and (11) and doing some lengthy integrals the general dispersion relation becomes

$$\frac{k^2 c^2}{\omega^2} = 1 + \frac{\omega_p^2}{\omega \beta^2 P_{o\perp}^{2(j+1)} j!} \left[X_i \frac{\beta m_e \omega}{k_{||} P_{0||}} Z(\xi) + X_2 (1 + \xi Z(\xi)) - X_5 \frac{\omega^2}{k^2 c^2} (1 + \xi Z(\xi)) \right] \tag{13}$$

where,

$$\begin{aligned} X_1 &= P_{o\perp}^{2(j+1)} - \frac{\upsilon \Gamma_x m_e}{\left(\frac{\omega_c}{\beta}\right)^2 - \upsilon^2} \left(j - \frac{1}{2}\right)! P_{o\perp}^{2j+1} \\ X_2 &= j! P_{o\perp}^{2(j+1)} \left(\frac{P_{o\perp}^2}{P_{o||}^2} (j+1) - 1 \right) - \frac{\upsilon \Gamma_x m_e}{\left(\frac{\omega_c}{\beta}\right)^2 - \upsilon^2} \left(j - \frac{1}{2}\right)! P_{o\perp}^{2j+1} \times \left(\frac{P_{o\perp}^2}{P_{o||}^2} (j+1) - 1 \right) \end{aligned}$$

$$X_5 = \frac{P_{o\perp}^2}{P_{o||}^2}\left[(j+1)!P_{o\perp}^{2(j+1)} - \frac{\upsilon\Gamma_x m_e}{\left(\frac{\omega_c}{\beta}\right)^2 - \upsilon^2}\left(j+\frac{1}{2}\right)!P_{o\perp}^{2(j+1)}\right]$$

$$\xi = \frac{\beta m_e\omega - m_e\omega_c + \beta m_e\upsilon}{k_{||}P_{o||}}$$

For real k and substituting $k^2c^2/\omega^2 \gg 1$, using an asymptotic expansion of $Z(\xi)$ in the limit of a large value of ξ, for $\omega = \omega_r + i\gamma$.

The expression for dimensionless growth rate and real frequency is found to be

$$\frac{\gamma}{\omega_c} = \frac{\frac{\sqrt{\pi}}{\tilde{k}\beta}\left(\frac{X_2}{X_1} - k_3\right)k_4^3\exp\left\{-\left(\frac{k_4}{\tilde{k}}\right)^2\right\}}{1+\beta X_4 + \frac{\tilde{k}^2}{2}\left(\frac{1+\beta X_4}{k_4^2} + \frac{2X_5\beta X_3 P_{o||}^2}{X_1\tilde{k}c^2}\right) - \frac{\tilde{k}^2}{k_4}\left(\frac{X_2}{X_1} - k_3\right)} \tag{14}$$

$$X_3 = \frac{k^2}{\beta_1}\left[k_2\left(1+\beta X_4\right) + \frac{X_2}{X_1}\frac{\beta_1}{1+\beta X_4}\right]$$

where the dimensionless growth rate and real frequency are defined as $\frac{\gamma}{\omega_c}$ and $X_3 = \frac{\omega_r}{\omega_c}$ respectively.

If relativistic factor $\beta = \sqrt{1-\frac{\upsilon^2}{c^2}}$ is ignored, the Equation (14) reduces to expression of non-relativistic growth rate, comparable to work done by Pandey and Kaur [23] using bi-Maxwellian distribution function.

Where

$$k_3 = \frac{\beta X_3}{k_4} + \frac{X_5}{X_1}\frac{\beta^2 X_3^2}{\tilde{k}^2}\frac{P_{o||}^2}{c^2}, \quad \tilde{k} = \frac{k_{||}P_{o||}}{m_e\omega_c}, \quad k_4 = 1 - \beta X_3 + \beta X_4,$$
$$X_4 = \frac{\omega'}{m_e\omega_c}, \quad \omega' = m_e\beta\upsilon, \quad \beta_1 = \frac{k_B T_{||}\mu_0 n_0}{B_0^2} \tag{15}$$

3. PLASMA PARAMETERS

To study the variation of dimensionless growth rate of whistler mode waves for non-relativistic background plasma for distribution index strength $j = 0$. The external injection of hot energetic electrons is considered to be relativistic and of loss-cone distribution index strength $j = 1$.

Non-relativistic bi-Maxwellian background plasma $j = 0$ has the following parameters: Temperature anisotropy $(A_T) = 0.25$, 0.50 and 0.75, Thermal energy $(K_B T_{ll}) = 10\,\text{eV}$, Electron density $(n_c) = 5\times10^4\,\text{m}^{-3}$, AC frequency $(\upsilon) = 6\,\text{Hz}$, 12 Hz and 18 Hz. Calculations have been performed with reported magnetic field of magnitude $B_o = 2.4\times10^{-10}\,\text{T}$ and magnitude of AC electric field $E_o = 4\,\text{mV/m}$. [23]

Relativistic injected warm plasma $j = 1$ has the following parameters: Temperature anisotropy $(A_T) = 0.25$, Thermal energy $(K_B T_{ll}) = 50\,\text{eV}$, Electron density $(n_c) = 2.5\times10^3\,\text{m}^{-3}$, $5\times10^3\,\text{m}^{-3}$ and $1.5\times10^3\,\text{m}^{-3}$, no AC frequency, Relativistic factor $(\upsilon/c) = 0$, 0.3 and 0.6. The external artificial beam is assumed to consist of fixed anisotropy and thermal energy. Electron density and velocity of the beam is considered variable. As the beam particles are not accelerated by any external electric field therefore, no AC frequency is assumed. One of the objective of this work is to study the behavior of energetic particles in presence of variable AC frequency of the background plasma. This variable AC frequency of the background plasma is due to AC field in the Uranian magnetosphere as observed by Voyager 2. Therefore, AC field is a property of the Uranus environment.

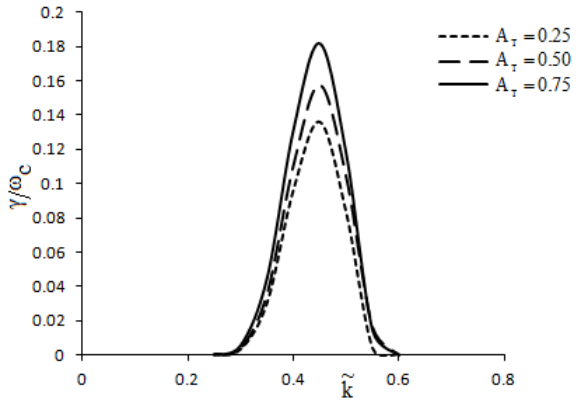

Figure 1. Variation of relativistic growth rate with $\tilde{k}$ for various values of temperature anisotropy in background plasma with $\upsilon = 6\,\mathrm{Hz}$ and $n_c/n_w = 10$.

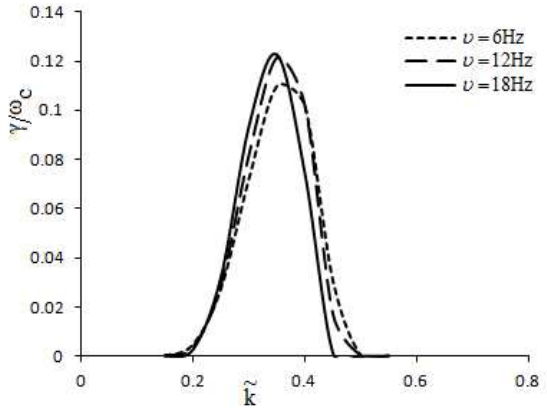

Figure 2. Variation of relativistic growth rate with $\tilde{k}$ for various values of AC frequencies for $A_T = 0.50$ and $n_c/n_w = 10$.

4. RESULT AND DISCUSSIONS

Figure 1 shows the variation of growth rate with respect to $\tilde{k}$ for various values of temperature anisotropy A_T and other fixed parameters as listed in figure caption. The anisotropy of 0.25, 0.50 and 0.75 is only for the background, with fixed anisotropy for the energetic particles. The growth rate is 0.136, 0.157 and 0.181 for $A_T = 0.25$, 0.50 and 0.75 respectively at $\tilde{k} = 0.45$. As the value of A_T increases, growth rate increases. Therefore it can be concluded that in case of injection of a distribution of particles having a positive slope in $v_\perp$, temperature anisotropy remains as the main source of free energy. As the distribution function of injected particles introduces a major change due to variation of thermal velocity [14, 24].

In Figure 2 variation of relativistic growth rate with $\tilde{k}$ for various values of AC frequencies is shown. Other parameters are fixed as mentioned in figure caption. The growth rate is 0.110, 0.121 and 0.122 for $\upsilon = 6\,\mathrm{Hz}$, $12\,\mathrm{Hz}$ and $18\,\mathrm{Hz}$ respectively at $\tilde{k} = 0.35$. Growth rate increases with increase in AC frequency. The graph shows that when same energetic particles (without AC field effect) are injected in background plasma of higher AC frequency, growth rate increases. The perpendicular electric field modifies perpendicular velocity and contributes to energy exchange too. For $j = 1$ loss cone index of the beam, the source of free energy is not only temperature anisotropy but also increasing value of $v_\perp$ having greater positive slope. AC field affects the growth rate marginally in comparison to above mentioned source of free energy. The bandwidth decreases for higher value of frequencies. Lower value of maxima is fixed for all values of AC frequency but higher value of wave number changes. The growth rate is mainly governed by dispersion function, which comprises of AC frequency as the most important component. In case of parallel electric field, dispersion function contains AC field magnitude as well as frequency, but in case of perpendicular electric field it contains frequency only [14, 25]. The energy exchange between the electrons, the component of wave electric field, electrons and the AC field perpendicular to magnetic field are the main factors contributing to cyclotron growth or the damping of waves.

Figure 3 shows the variation of dimensionless growth rate with $\tilde{k}$ for various values of ratio of number density of cold electrons to hot electrons. The number density of relativistic beam of hot electrons is varied as $5 \times 10^3\,\mathrm{m}^{-3}$, $2.5 \times 10^3\,\mathrm{m}^{-3}$ and $1.5 \times 10^3\,\mathrm{m}^{-3}$, thus giving n_c/n_w as 10, 20 and 30 (approximately). The growth rate is 0.136 for $\mathrm{n_c/n_w}$ =10 at $\tilde{k} = 0.45$, the growth rate is 0.094 when $n_c/n_w = 20$ at $\tilde{k} = 0.40$ and growth rate is $\gamma/\omega_c = 0.051$ for $n_c/n_w = 30$ at $\tilde{k} = 0.35$. This shows that as the number density of hot electrons increases, that is, as the ratio of n_c/n_w decreases from 30 to 10, growth rate increases. The corresponding $\tilde{k}$ value shifts from 0.35 to 0.45. This behavior is similar to the results quoted by Misra and Pandey [25] where studies were performed for magnetosphere of

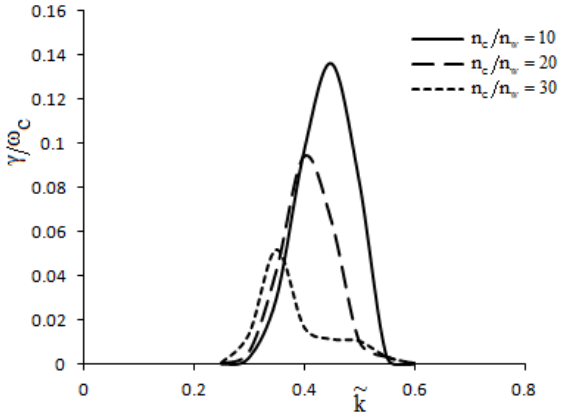

Figure 3. Variation of relativistic growth rate with $\tilde{k}$ for various values of ratio of number density of cold electrons to hot electrons having $\upsilon = 6\,\mathrm{Hz}$ and $A_T = 0.50$.

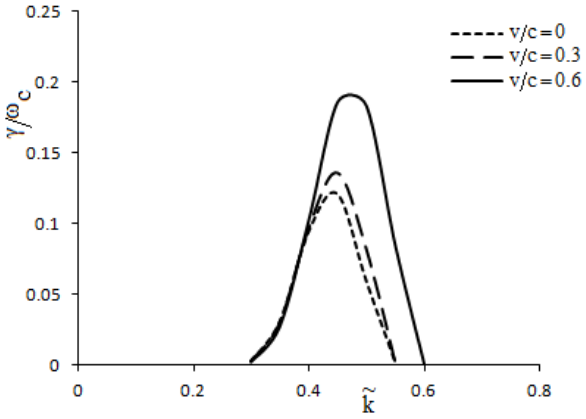

Figure 4. Variation of relativistic growth rate with $\tilde{k}$ for various values of relativistic factor at $\upsilon = 6\,\mathrm{Hz}$, $n_c/n_w = 10$ and $A_T = 0.50$.

Earth. So we learn that even the minimal presence of such energetic particles having a positive slope of distribution function and increasing the power of perpendicular thermal velocity increases the growth rate significantly.

Figure 4 shows the variation of dimensionless growth rate with respect to $\tilde{k}$ for various values of relativistic factor v/c and other fixed parameters as listed in figure caption. The growth rate is 0.120 for $v/c = 0$ at $\tilde{k} = 0.45$, the growth rate is 0.136 when $v/c = 0.3$ at $\tilde{k} = 0.45$ and growth rate is $\gamma/\omega_c = 0.186$ for $v/c = 0.6$ at $\tilde{k} = 0.45$. It is inferred that as the velocity of energetic electrons increases growth rate increases but band width is not shifted. Growth rates are very sensitive to the velocity spread as mode instability is a matter of wave particle resonance [26]. But the parallel momentum spread eventually results in a small velocity spread in case of a relativistic beam. So the waves tend to see a cold beam in parallel direction.

5. CONCLUSION

The effect of relativistic hot electron beam for field aligned Whistler mode waves has been studied in this paper. The theoretical analyses are based on the assumption of axial symmetry, in the presence of perpendicular AC electric field to magnetic field. Growth rate increases with increase in AC frequency. Although the effect of AC frequency is to trigger the instability, but calculations revealed that it also affects the growth rate. Studies have been performed using perturbative approach along with the method of characteristic solutions and are valid for comparatively small ambient magnetic field of Uranus, of the order of nano Tesla, as observed by Voyager 2. Results explain that temperature anisotropy remains as the main source of free energy when injection of a distribution of particles having a positive slope is considered. It is shown that even the minimal presence of energetic particles increases the growth rate significantly, as the number density of hot electrons increases, that is, as the ratio of n_c/n_w decreases, growth rate increases. Variation of relativistic factor v/c concludes that as the velocity of energetic electrons increases growth rate increases for magnetosphere of Uranus. This theoretical study of injection of hot electrons can be useful for studying the radiation belt particles and natural environment around Uranus.

ACKNOWLEDGMENT

The authors are thankful to Chairman, Indian Space Research Organisation (ISRO), Director and members of RESPOND program, ISRO, for constant support and research grants.

REFERENCES

1. Stix, T. H., *The Theory of Plasma Waves,* McGraw-Hill Book Company, New York, 1962.
2. Sagdeev, R. Z. and A. A. Galeev, *Non-linear Plasma Theory,* W. A. Benjamin, Inc. Book Company, New York City, NY, 1969.
3. Scarf, F. L. and D. A. Gurnett, "A plasma wave investigation for the Voyager mission," *Space Sci. Rev.*, Vol. 21, 289–308, 1977.
4. Gurnett, D. A. and F. L. Scarf, *Physics of Jovian Magnetosphere,* A. J. Dessler (ed.), 285, Cambridge University Press, Cambridge, 1983.
5. Lin, N., P. J. Kellogg, J. P. Thiessen, D. Lengyel-Frey, B. T. Tsurutani, and J. L. Phillips, "Whistler mode waves in the Jovian magnetosheath," *J. Geophys. Res.*, Vol. 99, No. A12, 23527–23540, 1994.
6. Hobara, Y., S. Kanemaru, M. Hayakawa, and D. A. Gurnett, "On estimating the amplitude of Jovian whistlers observed by Voyager 1 and implications concerning lightning," *J. Geophys. Res.*, Vol. 102, No. A4, 7115–7125, 1997.
7. Kurth, W. S., D. A. Gurnett, A. M. Persoon, A. Roux, S. J. Bolton, and C. J. Alexander, "The plasma wave environment of Europa," *Planet. Space Sci.*, Vol. 49, Nos. 3–4, 345–363, 2001.
8. Kurth, W. S., D. A. Gurnett, and F. L. Scarf, "Sporadic narrowband radio emissions from Uranus," *J. Geophys. Res.*, Vol. 91, No. 11, 11958–11964, 1986.
9. Orlowski, D. S. and C. T. Russell, "Comparison of properties of upstream whistlers at different planets," *Adv. Space Res.*, Vol. 16, 137–141, 1995.
10. Gurnett, D. A., F. L. Scarf, W. S. Kurth, and R. L. Poynter, "First plasma wave observation at Uranus," *Science*, Vol. 233, No. 4759, 106–109, 1986.
11. Ness, N. F., M. H. Acuna, K. W. Behannon, L. F. Burlaga, J. E. P. Connerney, R. P. Lepping, and F. M. Neubauer, "Magnetic fields at Uranus," *Science*, Vol. 233, No. 4759, 85–89, 1986.
12. Hudson, M. K., J. T. Clark, and J. A. Warren, "Ionospheric dynamo theory for production of far ultraviolet emissions on Uranus," *J. Geophys. Res.*, Vol. 94, 6517–6522, 1989.
13. Clarke, J. T., M. K. Hudson, and Y. L. Yung, "The excitation of the far ultraviolet eclectroglow emission on Uranus, Saturn and Jupiter," *J. Geophys. Res.*, Vol. 92, No. A13, 15139–15147, 1987.
14. Pandey, R. P., K. M. Singh, and R. S. Pandey, "A theoretical study of the whistler mode instability at the Uranian bow shock," *Earth, Moon and Planets*, Vol. 87, No. 2, 59–71, 2001.
15. Wygant, J. R., M. Bensadoum, and F. S. Mozer, "Electric field measurements at subcritical oblique bow shock crossings," *J. Geophys. Res.*, Vol. 92, No. A10, 11109–11121, 1987.
16. Winckler, J. R., P. R. Malcolm, R. L. Arnoldy, W. J. Burke, K. N. Erickson, J. Ernstmeyer, R. C. Franz, T. J. Hallinan, P. J. Kellogg, S. J. Monson, K. A. Lynch, G. Murphy, and R. J. Nemzek, "ECHO 7: An electron beam experiment in magnetosphere," *Eos, Transactions American Geophysical Union*, Vol. 70, No. 25, 657–668, 1989.
17. Winckler, J. R., "The application of artificial electron beams to magnetospheric research," *Reviews of Geophysics*, Vol. 18, No. 3, 659–682, 1980.
18. Winglee, R. M. and P. J. Kellogg, "Electron beam injection during active experiments: Electromagnetic wave emissions," *J. Geophys. Res.*, Vol. 95, No. A5, 6167–6190, 1990.
19. Pandey, R. P., S. M. Karim, K. M. Singh, and R. S. Pandey, "Effect of cold plasma injection on whistler mode instability triggered by perpendicular AC electric field at Uranus," *Earth, Moon and Planets*, Vol. 91, No. 4, 195–207, 2003.
20. Misra, K. D. and R. S. Pandey, "Generation of whistler emissions by injection of hot electrons in the presence of a perpendicular as electric field," *J. Geophys. Res.*, Vol. 100, No. A10, 19405–19411, 1995.
21. Sazhin, S. S., "Oblique whistler mode growth and damping in a hot anisotropic plasma," *Planet Space Science*, Vol. 36, 663–667, 1988.
22. Chu, K. R. and J. L. Hirshfield, "Comparitive study of the axial and azimuthal bunching mechanism in electromagnetic cyclotron instability," *Phys. Fluid*, Vol. 21, 461, 1978.

23. Pandey, R. S. and R. Kaur, "Generation of low frequency electromagnetic wave by injection of cold electron for relativistic and non-relativistic subtracted bi-Maxwellian distribution with perpendicular AC electric field for magnetosphere of Uranus," *Progress In Electromagnetic Research B*, Vol. 45, 337–352, 2012.
24. Pandey, R. S., K. Rajbir, S. Kumar, and K. Mukesh, "Study of VLF mode instability with AC electric field for subtracted bi-Maxwellian in the magnetosphere of Uranus," *J. Emerging Trends in Eng. and Applied Sci.*, Vol. 4, No. 2, 201–206, 2013.
25. Misra, K. D. and T. Haile, "Effect of AC electric field on the whistler mode instability in the magnetosphere," *J. Geophys. Res.*, Vol. 98, No. A6, 9297–9305, 1993.
26. Bret, A., M. C. Firpo, and C. Deutsch, "Electromagnetic instabilities for relativistic beam-plasma interaction in whole k space: Nonrelativistic beam and plasma temperature effects," *Phys. Review E*, Vol. 7, 016403, 2005.